10.1515/astro-2017-0228

Baltic Astronomy, vol. 24, 277–291, 2015

BARYON PHYSICS AND THE MISSING SATELLITES PROBLEM

A. Del Popolo[1,2,3]

[1] *Dipartimento di Fisica e Astronomia, University Of Catania, Viale Andrea Doria 6, 95125 Catania, Italy*

[2] *INFN sezione di Catania, Via S. Sofia 64, I-95123 Catania, Italy*

[3] *International Institute of Physics, Universidade Federal do Rio Grande do Norte, 59012-970 Natal, Brazil*

Received: 2015 July 3; accepted: 2015 September 10

Abstract. In the present paper, we combine the model of Del Popolo (2009) with the models dealing with tidal stripping, tidal heating, and photo-heating to study how baryon physics can solve the missing satellite problem (MSP) and the too-big-to-fail (TBTF) problem. Applying to the Via Lactea II (VL2) subhaloes a series of corrections similar to those of Brooks et al. (2013), namely, a Zolotov et al. (2012)-like correction obtained with our model, and further correcting for the UV heating and tidal stripping, we find that the number of massive and luminous satellites is in agreement with that number observed in the Milky Way. In conclusion, baryon physics is of fundamental importance in solving the ΛCDM small scale problems.

Key words: cosmology: theory – cosmology: large-scale structure of universe – galaxies: formation

1. INTRODUCTION

It is nowadays clear that despite the large success of the ΛCDM model at large scales (Spergel et al. 2003; Komatsu et al. 2011; Del Popolo 2007, 2013, 2014), small scales represent a problem for the paradigm quoted in a number of papers (e.g., Moore 1994; Moore et al. 1999; Ostriker & Steinhardt 2003; Boylan-Kolchin et al. 2011, 2012; Oh et al. 2011; Del Popolo et al. 2014)[1]. In this paper, we deal with two of the small scale problems of the ΛCDM model, namely, the "missing satellites problem" (MSP) which refers to the discrepancy between the number of predicted subhalos in N-body simulations (Moore et al. 1999) and the one observed[2], and a peculiar aspect of the MSP dubbed "too-big-to-fail" (hereafter TBTF) problem.

[1] Other problems of the ΛCDM model are the cosmological constant problem (Weinberg 1989; Astashenok & Del Popolo 2012) and the "cosmic coincidence problem".

[2] For the Milky Way the difference is larger than an order of magnitude.

Concerning the MSP, Klypin et al. (1999) and Moore et al. (1999) noticed that numerical simulations predicted much more subhaloes in galactic and cluster haloes. The number of satellites having circular velocities larger than those of Ursa Minor and Draco were $\simeq 500$, while it is well known that the Milky Way (MW) dSphs are much less numerous – nine bright dSphs (Boylan-Kolchin et al. 2012), Sagittarius, the LMC and the SMC. Subsequent cosmological simulations, such as Aquarius, VL2, and GHALO (Springel et al. 2008; Stadel et al. 2009; Diemand et al. 2007), confirmed the problem.

The MSP has recently shown another feature, while analyzing the Aquarius and the Via Lactea simulations. The simulated haloes have $\simeq 10$ (Boylan-Kolchin et al. 2011, 2012) subhaloes too massive and dense to host the MW brightest satellites. While ΛCDM simulations predict at least 10 subhaloes having $V_{\rm max} > 25\ {\rm km\,s^{-1}}$, the dSphs of the MW all have $12 < V_{\rm max} < 25\ {\rm km\,s^{-1}}$, implying a discrepancy between the simulations and the dynamics of the MW brightest dSphs (Boylan-Kolchin et al. 2011, 2012). This feature of the MSP problem has been dubbed the TBTF problem.

Two main classes of solutions have been proposed to the quoted problems: cosmological and astrophysical. Cosmological solutions are based on modifying the power spectrum at small scales (e.g. Zentner & Bullock 2003) or modifying the constituent particles of DM (e.g., Colin et al. 2000). Otherwise, modified gravity theories, like $f(R)$ (Buchdal 1970; Starobinsky 1980), $f(T)$ (see Ferraro 2012), and MOND (Milgrom 1983a,b), can solve the problem.

Astrophysical solutions are usually connected to baryon physics and consider:

(a) the change of shape of satellites from cuspy to cored[3] (e.g., Del Popolo 2009 (DP09); Zolotov et al. 2012 (Z12); Brooks et al. 2013 (B13)), which makes the satellites more subject to tidal stripping effects and even subject to being destroyed (Strigari et al. 2007; Peñarrubia et al. 2010). In this picture, the present-day dwarf galaxies could have been more massive in the past, and they were transformed and reduced to their present "status" by strong tidal stripping (e.g., Kravtsov et al. 2004);

(b) Suppression of star formation due to supernova feedback (SF), photoionization (Okamoto et al. 2008; B13), and reionization. In particular, reionization can prevent the acquisition of gas by DM haloes of small mass, then "quenching" star formation after $z \simeq 10$ (Bullock et al. 2000; Ricotti & Gnedin 2005; Moore et al. 2006). This would suppress dwarfs formation or could make them invisible;

(c) Effects of a baryonic disk (Z12; B13). Disk shocking produces strong tidal effects on the satellites passing through the disk, which are stronger if the satellite has a cored inner profile.

The previous discussion shows that the small scale problems can be solved appropriately taking into account the baryon physics. A trial to find unifying baryon solutions to the small scale problems is that of Z12 and B13. In Z12 it was shown that the same model can solve the TBTF. Z12 found a correction to the

[3] The cusp to core transformation is obtained through two different mechanisms: (a) "supernova-driven flattening " (Navarro et al. 1996; Gelato & Sommer-Larsen 1999; Read & Gilmore 2005; Mashchenko et al. 2006, 2008; Governato et al. 2010; Pontzen & Governato 2012), in which supernovae explosions erase the cusp; (b) dynamical friction from baryonic clumps (El-Zant et al. 2001, 2004; Romano-Diaz et al. 2008; Del Popolo 2009; Del Popolo & Kroupa 2009; Cole et al. 2011), in which model transfer of energy and angular momentum from DM to baryons eliminates the cusp.

velocity in the central kiloparsec of galaxies to mimic the flattening of the cusp due to SF, and the enhancement of tidal stripping produced by a baryonic disk. This correction, together with destruction effects produced by the tidal field of the baryonic disk, and the identification of subhaloes that remain dark because of inefficiency in forming stars due to UV heating, were applied by B13 to the subhaloes of the VL2 simulation (Diemand et al. 2008). As a result, the number of massive subhaloes in the VL2 appeared to be in agreement with the number of satellites of the MW.

In the present paper, we study through the model of DP09 if the MSP and the TBTF problem can be simultaneously solved using baryon physics. The main goal of this paper is to see how baryon physics changes the number and mass of the satellites of the MW. This aim will be followed correcting the VL2 simulations for the baryon physics effects which VL2 do not take into account. As better discussed in the following sections, the baryons effect taken into account consists of (a) flattening of the density profile which is calculated with the DP09 model; (b) tidal stripping, tidal heating and photo-heating, taken into account as discussed in §2.2. As we will see, the quoted corrections are able to solve simultaneously two big problems of the ΛCDM model, whose solution is necessary in order to save the predictive power of the ΛCDM model itself.

The paper is organized as follows. In Section 2, we summarize the model, Section 3 describes the future study plans connected to the present paper, and Section 4 is devoted to conclusions.

2. THE MISSING SATELLITES AND THE TOO-BIG-TO-FAIL PROBLEMS

As reported, the MSP concerns the incorrect prediction of simulations of the subhaloes distribution in structures or satellites of our MW. The TBTF problem is a peculiar feature of the MSP, which shows that subhalos in a DM-only simulation have significantly higher central densities than inferred from observations of the Milky Way's classical dwarf spheroidal satellites.

Several solutions have been proposed to both problems (Strigari et al. 2007; Simon & Geha 2007; Madau et al. 2008; Z12; Purcell & Zentner 2012; Vera-Ciro et al. 2013; Wang et al. 2012; Brooks & Zolotov 2014).

An interesting baryonic solution to the MSP and the TBTF problem was proposed by B13. The main idea is that, instead of running very time consuming SPH simulations of different galaxies, one can introduce the baryons effect in large N-body dissipationless simulations, like VL2, showing that the result obtained is in agreement with observations of the MW and M31 satellites.

In the following, we will partly follow their steps to obtain the corrected circular velocities and distribution of VL2 satellites in the framework described by DP09 (see, also, the Appendix).

In summary, our method is based on the following ideas and is divided into two main phases.

2.1. First phase: cusp erasing

Initially the attention is directed to the isolated satellites, before their accretion to the main system. As noticed by several authors (e.g., Mashchenko et al. 2006, 2008; Peñarrubia et al. 2010) the effects of the tidal forces of the main halo on a satellite depends fundamentally on its shape. If the satellite has a cuspy profile,

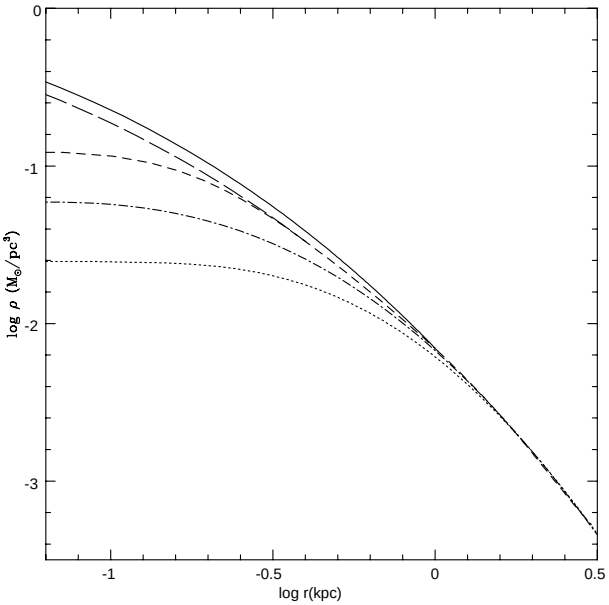

Fig. 1. Density profile evolution of a $10^9 M_\odot$ halo with baryon fraction $f_{\rm d} \simeq 0.04$ and a specific angular momentum $h \simeq 400$ kpc km s^{-1} ($\lambda \simeq 0.05$), starting from $z = 10$ (solid line), when the profile is a NFW profile. The following evolution represented by the long-dashed line, short-dashed line, dot-dashed line, dotted line represents the profile at $z = 3, 2, 1, 0$, respectively.

tidal torques will not impart big changes to its structure when it will enter the main halo. If the satellite has a cored profile, the tidal field of the main halo can strip easily its gas and, in some cases, even destroy it (Peñarrubia et al. 2010). Therefore, this first phase, defining the shape of the satellite, is of fundamental importance. This first phase and the flattening of the satellites density profiles will be studied through our model.

We now show how the model of DP09 (see also the Appendix) can solve the quoted problems. As done in previous papers, DP09, Del Popolo (2012a,b, hereafter DP12a,b), Del Popolo & Hiotelis (2014), we will study the evolution of protostructures from the linear phase until they form structures with galactic mass, and then we calculate their density profiles, and the DM and baryon angular momentum distribution. Then we find, similarly to Z12, an analytical correction to apply to the center of the haloes which mimics the effect of flattening of the cusp, and, similarly to B13, we apply the previous correction, together with the tidal destruction and UV heating effects on subhaloes, to the VL2 simulations (as done by B13).

Fig. 1 shows the evolution of a $10^9 M_\odot$ halo with specific angular momentum chosen to be similar to that of a typical late-type dwarf galaxy (e.g., UGC 6446, see van den Bosch et al. 2001; Cardone & Del Popolo 2012), namely $h \simeq 400$ kpc km s^{-1} ($\lambda \simeq 0.05$), and the baryon fraction (see the Appendix) $f_{\rm d} \simeq 0.04$. Evolution starts from the redshift of virialization $z = 10$ (solid line). The density profiles at $z = 3$, 2, 1 and 0 are represented by the long-dashed line, short-dashed line, dot-dashed line and dotted-line, respectively. The final density profile is well

described by a Burkert profile (Burkert 1995).

The proto-structure and profile evolution is summarized in the Appendix. After virialization the density profile evolution is due to secondary infall, two-body relaxation, interplay between DM and baryons. As shown in Fig. 1, the profile flattens and a core is formed within 1 kpc (Del Popolo et al. 2013a). A similar result was obtained by Romano-Diaz et al. (2008), who performed N-body simulations of the DM density profile in the absence and in the presence of baryons. Cusp erasing was connected by them to an influx of sub-haloes in the central part of the halo, as well as to heating up of DM through dynamical friction (DF), similarly to the El-Zant et al. (2001, 2004) results. Concerning the model proposed by El-Zant et al., it is based on baryonic clumps which exchange angular momentum through dynamical friction with DM. As previously reported, there is observational evidence on the existence of these clumps, coming from high-z observations of galaxies (Elmegreen et al. 2004, 2009; Genzel et al. 2011). These clumps are of fundamental importance in the formation of bulges, in the so-called "clump-origin bulge" (Noguchi 1998, 1999; Inoue & Saitoh 2011). As it has been shown by Inoue & Saitoh (2011) through SPH simulations, these clumps are able to flatten the cuspy profile.

Theoretical results which are in agreement with the previous ones were reported in several papers (El-Zant et al. 2001, 2004; Ma & Boylan-Kolchin 2004; Romano-Diaz et al. 2008; Cole et al. 2011, Nipoti & Binney 2015). The results were also compared and found in agreement with the SPH simulations of Governato et al. (2010), in DP12a. Recently, Polisenky & Ricotti (2015) also confirmed the results of the model through N-body simulations.

Our result for the flattening of the density profile is expressed in terms of the change to circular velocity in 1 kpc, as in Z12, by calculating the difference between the satellites DM-only rotation velocity in 1 kpc and that of the satellites with baryons plus DM. The result is

$$\Delta(v_{1\,\mathrm{kpc}}) \;=\; 0.3\, v_{\mathrm{infall}} - 0.2\ \mathrm{km\,s^{-1}}, \tag{1}$$

in the interval $20\ \mathrm{km\,s^{-1}} < v_{\mathrm{infall}} < 50\ \mathrm{km\,s^{-1}}$. The above correction is determined for the Z12 satellites, and it will be applied to the VL2 satellites, together with other corrections to be discussed in this paper. The correction that we obtained is close to that obtained by Z12, accounting mainly for the reduction of the subhaloes central mass produced by SF and given by

$$\begin{aligned}\Delta(v_{1\,\mathrm{kpc}}) \;&=\; 0.2\, v_{\mathrm{infall}} - 0.26\ \mathrm{km\,s^{-1}},\\ &\qquad 20\ \mathrm{km\,s^{-1}} < v_{\mathrm{infall}} < 50\ \mathrm{km\,s^{-1}}.\end{aligned}$$

The previous equation gives the corrections to apply to satellites in N-body simulations that take into account the missing piece of baryonic physics.

The above corrections give rise to a reduction of the circular velocities. Comparing with Z12 result, we have that, in the case of $v_{\mathrm{infall}} = 30\ \mathrm{km\,s^{-1}}$, the Z12 correction gives $\Delta(v_{1\mathrm{kpc}}) = 5.74\ \mathrm{km\,s^{-1}}$, while our correction gives $\Delta(v_{1\mathrm{kpc}}) = 8.8\ \mathrm{km\,s^{-1}}$. The difference between the $\Delta(v_{1\mathrm{kpc}})$ value of our model and that of Z12 is due to the different models used to produce the pre-infall flattening of the satellites density profile. The final reduction of the quoted velocities after taking into account tidal stripping (see the next subsection) can be directly read from Fig. 2. The top panel in Fig. 2 shows the circular velocity obtained in VL2 dissipationless

N-body simulations, while the bottom one shows the velocities after all the corrections discussed are taken into account. This velocity difference is produced by the additive effects of density profile flattening, tidal stripping and heating, and photo-ionization, which are not taken into account in the VL2 simulations.

If we look at the top point in the top panel of Fig. 2, the velocity of the satellite in DM-only simulations is 36.5 $\mathrm{km\,s^{-1}}$, while after the quoted corrections applied it reduces to 25 $\mathrm{km\,s^{-1}}$. As we discussed at the beginning, this brings the velocity into agreement with observations (recall that the dSphs of the MW all have $12 < V_{\rm max} < 25$ $\mathrm{km\,s^{-1}}$).

The difference among our model and that used in Z12 is in the model used to calculate the pre-infall flattening. In Z12 the pre-infall flattening is due to SF, while in our case it is connected to dynamical friction. As shown by Cole et al. (2011), DF on infalling clumps is a very efficient mechanism in flattening the DM profile. A clump having a mass of 1% of the halo mass can give rise to a core from a cuspy profile removing two times its mass from the inner part of the halo. In the case of the SF the mechanism should be less effective going down to lower masses (e.g., dwarfs with stellar mass $< 10^5 - 10^7 M_\odot$ have few stars and, as a consequence, supernovae explosions are relatively rare events).

2.2. Second phase: satellites interacting with the main halo

Then comes the second phase, when the satellite is no longer considered isolated, there being subject to the tidal field of the main halo, and, finally, it is accreted to the main halo (see the following).

Our correction (Eq. 1), similarly to the Z12 correction, applies to satellites that survived at $z = 0$ and which had the central $V_{\rm c}$ reduced by baryonic physics. Before $z = 0$, satellites could have been destroyed (by, e.g., stripping or photo-heating). In N-body simulations, like in the VL2, baryons effects are not taken into account, and then satellites, that in the real universe or in SPH simulations may be totally destroyed by enhanced tidal stripping (due to disks and cores) and SF, will not be destroyed. Since our correction and that of Z12 apply to satellites that survived to z=0, not to those that were previously destroyed, we need two other corrections (tidal stripping and suppression of star formation), as in B13, to calculate the survived satellites and then to apply the Z12 correction.

Here starts the second phase mentioned above, with the effects of the interaction between the main halo and the satellite to be considered.

In order to get accurate $V_{\rm max}$ values when tidal stripping and tidal heating after infall are taken into account, we could follow the Taylor & Babul (2001) model (see the following) which includes the effect of tidal mass and that of tidal heating in an analytical manner. However, this will be done in a future paper, and here we estimate the effect of stripping after infall, adding two corrections (as done in B13).

The first of the two corrections is for the suppression of star formation by photo-heating, obtained following the Okamoto et al. (2008) results. The second one is for the destruction rates by stripping of satellites, obtained following Peñarrubia et al. (2010).

We will use Eq. 8 from Peñarrubia et al. (2010) for subhaloes with the density slope of dark matter, γ, to calculate

$$v_{\rm max}(z=0) = v_{\rm infall}\frac{2^\alpha x^\eta}{(1+x)^\alpha}, \tag{2}$$

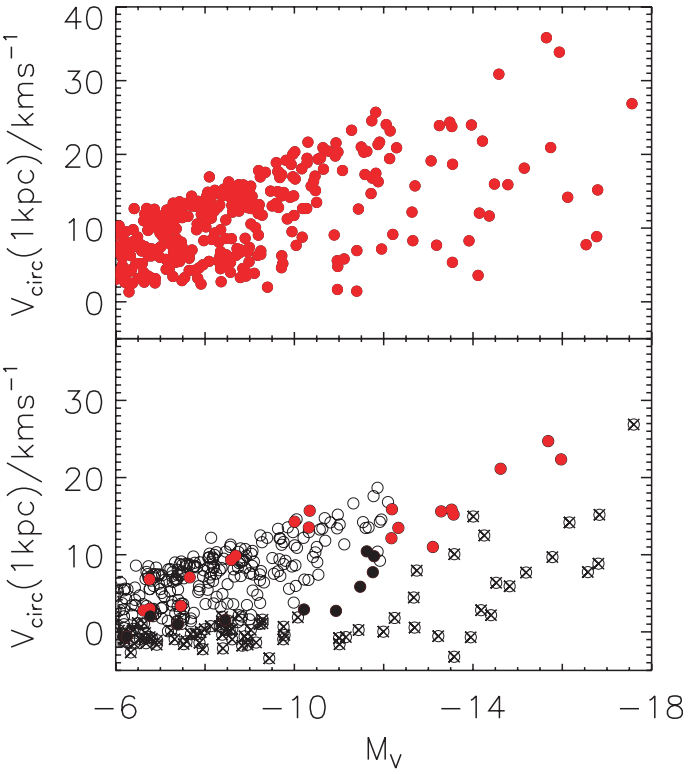

Fig. 2. Plot of $v_{1\mathrm{kpc}}$ vs. M_V for the VL2 simulation subhaloes. In the top panel, we plot the VL2 satellites at $z = 0$, as in B13. In the bottom panel, we represent the same VL2 satellites with the baryonic corrections (see the text) applied. The filled black circles represent satellites that have lost enough mass (stars are stripped and the luminosities are upper limits). Filled red circles are for satellites observed at $z = 0$, while circles with "x" denote subhaloes that have low probability to survive tidal effects. Dark subhaloes are represented by empty circles.

where $x \equiv \mathrm{mass}(z = 0)/\mathrm{mass}(z = \mathrm{infall})$ describes the change in V_{max} as a function of mass lost due to tidal stripping, and α and η are two fitting parameters whose values are connected to the slope γ as shown in Fig. 6 of Peñarrubia et al. (2010). For the DM-only runs, which have cuspy density profiles, $\gamma = -1$ gives a good fit to the change in V_{max}. Since the satellites have a profile that can be cored, we have chosen a value of γ in the range $\gamma = -0.5 - 0$ and values of α and η given by Peñarrubia et al. (2010, their Fig. 6). In the case of the VL2 satellites, the values of α and η are 0.4 and 0.3, respectively.

In order to use the equation quoted above, we need to know the mass lost in tidal stripping. Those values can be read from Fig. 6 in Z12. Then, we apply the Peñarrubia et al. (2010) equation to get the change in V_{max}. Assuming that V_{max} is approximately the same as $V_{1\mathrm{kpc}}$, we get the needed correction after infall.

Similarly to B13, (a) the population of satellites that loses more than 97% of their infall mass, and (b) all subhalos losing more than 90% of their infall mass, having also apocentric passages < 20 kpc and $v_{\mathrm{infall}} > 30\ \mathrm{km\,s^{-1}}$, are considered to be destroyed. Then, the subhaloes that remain dark because they are affected

by the UV heating and do not form stars are calculated using the Okamoto et al. (2008) SPH simulations and the results of Sect. 3.2 of B13.

Finally, we have to assign a luminosity to the satellites which survived. For this, we apply the relation between $v_{\rm infall}$ and the stellar mass M_*, obtained by Z12,

$$\Big(\frac{v_{\rm infall}}{\rm km\,s^{-1}}\Big)^6 = 55.56\frac{M_*}{M_\odot}. \tag{3}$$

By using the relation between M_* and the visual absolute magnitude M_V,

$$M_* = L_V \times 10^{-0.734+1.404(B-V)}, \tag{4}$$

where, according to Munshi et al. (2013),

$$L_V = 10^{-(V-4.8)/2.5}, \tag{5}$$

we approximate, as in B13, Eq.(3) to get

$$\log_{10}(\frac{M_*}{M_\odot}) = 2.37 - 0.38M_V. \tag{6}$$

The result produced by application of the corrections described is demonstrated in Fig. 2. The top panel of this figure shows the results from VL2 simulations at $z = 0$. The bottom panel represents the same VL2 satellites after the corrections discussed above (heating, destruction and velocity corrections) were applied. The red filled symbols denote the objects "observable" in VL2. Dark objects are plotted as empty circles. Objects indicated by circles with "x" represent subhaloes that do not survive due to the baryonic effects (e.g., baryonic disk, etc). Empty circles represent objects that have a mass smaller than the minimum mass to retain baryons and form stars. Finally, filled black circles denote satellites that have lost 90% of their mass since infall, but do not satisfy the destruction criteria described above.

Note that the Z12 correction was not applied to satellites with $v_{\rm max} > 50$ km s^{-1} (for example, to the satellites with $M_V < -16$, which are the five most massive satellites at infall and are the five that had $v_{\rm max} > 50$ km s^{-1}).

The number of satellites with $v_{\rm 1kpc} > 20$ km s^{-1} is, similarly to B13, equal to three. Our central velocities are smaller than those obtained by Z12 and B13. This is because in our model the correction to the circular velocity, $\Delta(v_{\rm 1kpc})$, is larger with respect to the values obtained by Z12 and B13.

As in B13, the Z12 correction is necessary in order to reconcile the masses of the subhaloes with observations, while the UV heating and tidal destruction are necessary to reconcile the total number of luminous satellites with observations.

3. FUTURE PLANS

In the present paper, we considered the evolution of satellites before infall and calculated, using our model, the flattening of the density profile (not the SF flattening effect), to which we added the further flattening (or reduction of the central rotation velocity) produced by the interaction with the main halo. This last step was based on the calculation of the flattening, after infall, shown in B13. In a forthcoming paper, we will improve the model as follows. We will calculate

again the profile flattening of satellites before infall as done in this paper, but then we will use a model like that of Taylor & Babul (2001) being able to follow the merger history and growth of the satellites while interacting with the main halo. By tracking the substructure evolution in the main halo (Del Popolo & Gambera 1997) and taking account of the mass loss due to tides, and tidal heating, we will have enough information to conclude if they are massive enough to retain baryons and form stars.

Since our model is not so computationally "heavy" as SPH simulations, we could study the MSP problem in different galaxies, since it is not enough to solve the problem in a single galaxy and to conclude that the problem is solved in galaxies different from ours. In fact, several authors have discussed the MSP problem in relation to the host galaxy mass. Vera-Ciro et al. (2013) and Wang et al. (2012) have shown that if the MW's true virial mass is smaller than $10^{12} M_{\odot}$, namely $\simeq 8 \times 10^{11} M_{\odot}$, the satellites excess may disappear.

In any case, the main point of our study is that baryonic physics is able to solve simultaneously the small scale problems of the ΛCDM model: cusp/core problem, MSP and TBTF problem.

A similar result has been obtained by a series of papers (Governato et al. 2010; Governato et al. 2012; Z12; Brooks & Zolotov 2014). In these papers, the main effect producing the flattening of the cusp, and the TBTF solution, are connected to the effects of SF, following episodic bursts of supernovae.

In our model, the solution to the previously quoted problems is connected to the complex interaction between DM and baryons mediated by DF. Our study is similar to those of El-Zant et al. (2001, 2004), Romano-Diaz et al. (2008), and Cole et al. (2011), in the sense that, like in their works, DF plays an important role. Differently from the previous studies, we consider the joint effect of several other effects (e.g., random angular momentum, angular momentum generated by tidal torques, adiabatic contraction, cooling, star formation), which in the quoted studies were not considered.

4. CONCLUSIONS

The main goal of this paper was to study the effect of baryon physics on the MSP and the TBTF problems. To this end, we used the VL2 DM-only simulations and studied how the predictions of such simulations are modified when we take into account: (a) the effect of the density profile flattening due to the presence of baryons, (b) tidal stripping and heating, and photo-ionization.

The study was divided into two phases. In the first one, we used the model of DP09 to see the effects of density profile flattening on VL2 predictions. More precisely, we studied through our DP09 model how baryons influence the inner density profile (or the inner circular velocity, $v_{1\mathrm{kpc}}$) before infall in the host halo. In the second phase, the interaction of infalling satellites on the main halo and, namely, the effects of tidal stripping and heating were studied following some results of Peñarrubia et al. (2010). The suppression of star formation by photo-ionization was obtained following Okamoto et al. (2008). Then, we added the changes to $v_{1\mathrm{kpc}}$ calculated in the first phase (pre-infall) to the changes to $v_{1\mathrm{kpc}}$ after infall, produced by tidal stripping and UV heating. After assigning a luminosity to the satellites that survived, we were able to plot circular velocities in terms of magnitude for the satellites given by DM-only simulations and for those corrected for

the baryon physics processes described.

The main result is demonstrated in Fig. 2. The plot shows the circular velocity in 1 kpc, $v_{1\mathrm{kpc}}$, in terms of the visual absolute magnitude for the satellites in the DM-only VL2 simulations (top panel) and for the satellites when the reported baryon physics effects are taken into account (bottom panel).

There are several important points to note in the bottom panel of the figure: (a) a noteworthy decrease in the circular velocity due to the density profile flattening produced in the pre-infall phase by the interaction of baryonic clumps and DM. The number of satellites with $v_{1\mathrm{kpc}} > 20\,\mathrm{km\,s^{-1}}$ in the VL2 simulations (top-panel) is 28, while after correcting for baryons effects it reduces to three in agreement with B13 and observations; (b) satellites shown by circles with "x" were destroyed in the interaction with the main halo due to tidal heating and stripping; (c) empty circles represent satellites that due to photo-ionization do not have enough gas to form stars and remain dark; (d) filled circles were subject to noteworthy stripping and their luminosities are upper limits.

The plot shows that baryon physics put the number of satellites and their central velocity, namely, their mass, in line with observations. This means that baryon physics is able to solve simultaneously the MSP and the TBTF problem. This is an important result, and the main result of this paper.

REFERENCES

Ascasibar Y., Yepes G., Gottlöber S. 2004, MNRAS, 352, 1109
Astashenok A. V., Del Popolo A. 2012, Class. Quantum Grav., 29, 085014
Avila Reese V., Firmani C., Hernandez X. 1998, ApJ, 505, 37
Bertschinger E. 1985, ApJS, 58, 39
Blumenthal G. R., Faber S. M., Flores R., Primack J. R. 1986, ApJ, 301, 27
Boylan-Kolchin M., Bullock J. S., Kaplinghat M. 2011, MNRAS, 415, 40
Boylan-Kolchin M., Bullock J. S., Kaplinghat M. 2012, MNRAS, 422, 1203
Brooks A. M., Zolotov A. 2014, ApJ, 786, 87
Brooks A. M., Kuhlen M., Zolotov A., Hooper D. 2013, ApJ, 765, 22 (B13)
Buchdahl H. A. 1970, MNRAS, 150, 1
Bullock J. S., Kravtsov A. V., Weinberg D. H. 2000, ApJ, 539, 517
Burkert A. 1995, ApJ, 447, L25
Cardone V. F., Del Popolo A. 2012, MNRAS, 427, 3176
Cardone V. F., Del Popolo A., Tortora C., Napolitano N. R. 2011a, MNRAS, 416, 1822
Cardone V. F., Leubner M. P., Del Popolo A. 2011b, MNRAS, 414, 2265
Catelan P., Theuns T. 1996, MNRAS, 282, 436
Chandrasekhar S. 1943, ApJ, 97, 255
Colin P., Avila-Reese V., Valenzuela O. 2000, ApJ, 542, 622
Cole D. R., Dehnen W., Wilkinson M. I. 2011, MNRAS, 416, 1118
De Lucia G., Helmi A. 2008, MNRAS, 391, 14
Del Popolo A. 2002, MNRAS, 337, 529
Del Popolo A. 2007, Astronomy Reports, 51, 169
Del Popolo A. 2009, ApJ, 698, 2093 (DP09)
Del Popolo A. 2010, MNRAS, 408, 1808
Del Popolo A. 2011, JCAP, 07, 014

Del Popolo A. 2012a, MNRAS, 424, 38 (DP12a)
Del Popolo A. 2012b, MNRAS, 419, 971 (DP12b)
Del Popolo A. 2013, Proceed. AIP Conf., 1548 , pp. 2–63
Del Popolo A. 2014, IJMPD, 23, 1430005
Del Popolo A., Gambera M. 1996, A&A, 308, 373
Del Popolo A., Gambera M. 1997, A&A, 321, 691
Del Popolo A., Gambera M. 1999, A&A, 344, 17
Del Popolo A., Gambera M. 2000, A&A, 357, 809
Del Popolo A., Hiotelis N. 2014, JCAP, 01, 047
Del Popolo A., Kroupa P. 2009, A&A, 502, 733
Del Popolo A., Cardone V. F., Belvedere G. 2013a, MNRAS, 429, 1080
Del Popolo A., Pace F., Lima J. A. S. 2013b, MNRAS, 430, 628
Del Popolo A., Pace F., Lima J. A. S. 2013c, IJMPD, 22, 1350038
Del Popolo A., Pace F., Maydaniuk S. P. et al. 2013d, Phys. Rev. D, 87, Issue 4, id. 043527
Del Popolo A., Lima J. A. S., Fabris J. C., Rodrigues D. C. 2014, JCAP, 04, 021
Di Cintio A., Brook C. B., Macció A. V. et al. 2014, MNRAS, 437, 415
Diemand J., Kuhlen M., Madau P. 2007, ApJ, 667, 859
Eisenstein D. J., Loeb A. 1995, ApJ, 439, 520
Elmegreen D. M., Elmegreen B. G., Hirst A. C. 2004, ApJ, 604, L21
Elmegreen D. M., Elmegreen B. G., Marcus M. T. et al. 2009, ApJ, 701, 306
El-Zant A., Shlosman I., Hoffman Y. 2001, ApJ, 560, 636
El-Zant A. A., Hoffman Y., Primack J. et al. 2004, ApJ, 607, L75
Ferraro R. 2012, Proceed. AIP Conf., 1471, 103 = arXiv:1204.6273v2
Fillmore J. A., Goldreich P. 1984, ApJ, 281, 1
Gelato S., Sommer-Larsen J. 1999, MNRAS, 303, 321
Genzel R., Newman S., Jones T. et al., 2011, ApJ, 733, 101
Gnedin O. Y., Kravtsov A. V., Klypin A. A., Nagai D. 2004, ApJ, 616, 16
Governato F., Brook C., Mayer L. et al. 2010, Nature, 463, 203
Governato F., Zolotov A., Pontzen A. et al. 2012, MNRAS, 422, 1231
Gunn J. E. 1977, ApJ, 218, 592
Gunn J. E., Gott J. R. 1972, ApJ, 176, 1
Gustafsson M., Fairbairn M., Sommer-Larsen J. 2006, Phys. Rev. D, 74, 123522
Hiotelis N., Del Popolo A. 2006, Ap&SS, 301, 167
Hiotelis N., Del Popolo A. 2013, MNRAS, 436, 163
Hoffman Y., Shaham J. 1985, ApJ, 297, 16
Hoyle F. 1949, in *Problems of Cosmological Aerodynamics* (IAU and International Union of Theorethical and Applied Mechanics Symposium), eds. J. M. Burgers & H. C. van de Hulst, Central Air Documents, Dayton, Ohio, p. 195
Inoue S., Saitoh T. R. 2011, MNRAS, 418, 2527
Kandrup H. E. 1980, Phys. Rept., 63, 1
Klypin A., Kravtsov A. V., Valenzuela O., Prada F. 1999, ApJ, 522, 82
Klypin A., Zhao H.-S., Somerville R. S. 2002, ApJ, 573, 597
Komatsu E., Dunkley J., Nolta M. R. et al. 2009, ApJS, 180, 330
Komatsu E., Smith K. M., Dunkley J. et al. 2011, ApJS, 192, 18
Kravtsov A. V., Gnedin O. Y., Klypin A. A. 2004, ApJ, 609, 482
Li Y.-S., De Lucia G., Helmi A. 2010, MNRAS, 401, 2036

Le Delliou M., Henriksen R. N. 2003, A&A, 408, 27
Ma C-P., Boylan-Kolchin M. 2004, Phys. Rev. Lett., 93, 021301
Madau P., Diemand J., Kuhlen M. 2008, ApJ, 679, 1260
Martizzi D., Teyssier R., Moore B., Wentz T. 2012, MNRAS, 422, 3081
Mashchenko S., Couchman H. M. P., Wadsley J. 2006, Nature, 442, 539
Mashchenko S., Wadsley J., Couchman H. M. P. 2008, Science, 319, 174
McGaugh S. S., Schombert J. M., de Blok W. J. G., Zagursky M. J. 2010, ApJ, 708, L14
Milgrom M. 1983a, ApJ, 270, 365
Milgrom M. 1983b, ApJ, 270, 371
Moore B. 1994, Nature, 370, 629
Moore B., Quinn T., Governato F. et al. 1999, MNRAS, 310, 1147
Moore B., Diemand J., Madau P. et al. 2006, MNRAS, 368, 563
Navarro J. F., Eke V. R., Frenk C. S. 1996, MNRAS, 283, L72
Newman A. B., Treu T., Ellis R. S. et al. 2013a, ApJ, 765, 25
Newman A. B., Treu T., Ellis R. S. et al. 2013b, ApJ, 765, 24
Nipoti C., Binney J. 2015, MNRAS, 446, 1820
Noguchi M. 1998, Nature, 392, 253
Noguchi M. 1999, ApJ, 514, 77
Oh S.-H., de Blok W. J. G., Brinks E. et al. 2011, AJ, 141, 193
Okamoto T., Gao L., Theuns T. 2008, MNRAS, 390, 920
Ostriker J. P., Steinhardt P. 2003, Science, 300, 1909
Peebles P. J. E. 1969, ApJ, 155, 393
Peebles P. J. E. 1980, *The Large Scale Structure of the Universe*, Princeton Univ. Press
Peñarrubia J., Benson A. J., Walker M. G. et al. 2010, MNRAS, 406, 1290
Polisenky E., Ricotti M. 2015, MNRAS, 450, 2172
Pontzen A., Governato F. 2012, MNRAS, 421, 3464
Purcell C. W., Zentner A. R. 2012, JCAP, 12, 7
Read J. I., Gilmore G. 2005, MNRAS, 356, 107
Ricotti M., Gnedin N. Y. 2005, ApJ, 629, 259
Romano-Diaz E., Shlosman I., Hoffman Y., Heller C. 2008, ApJ, 685, L105
Ryden B. S. 1988, ApJ, 329, 589
Ryden B. S., Gunn J. E. 1987, ApJ, 318, 15
Simon J. D., Geha M. 2007, AAS Meeting, 211, 26.02
Spedicato E., Bodon E., Del Popolo A., Mahdavi-Amiri N. 2003, 4OR, Vol. 1, Issue 1, 51
Spergel D. N., Verde L., Peiris H. V. et al. 2003, ApJS, 148, 175
Springel V., Wang J., Vogelsberger M. et al. 2008, MNRAS, 391, 1685
Stadel J., Potter D., Moore B. et al. 2009, MNRAS, 398, 21
Starobinsky A. A. 1980, Physics Letters B, 91, 99
Strigari L. E., Bullock J. S., Kaplinghat M. et al. 2007, ApJ, 669, 676
Taylor J. E., Babul A. 2001, ApJ, 559, 716
van den Bosch F. C., Burkert A., Swaters R. A. 2001, MNRAS, 326, 1205 (VBS)
Vera-Ciro C. A., Helmi A. Starkenburg E., Breddels M. A. 2013, MNRAS, 428, 1696
Wang J., Frenk C. S., Navarro J. F. et al. 2012, MNRAS, 424, 2715

Weinberg S. 1989, Rev. Mod. Phys., 61, 1
White S. D. M. 1984, ApJ, 286, 38
White S. D. M., Zaritsky D. 1992, ApJ, 394, 1
Williams L. L. R., Babul A., Dalcanton J. J. 2004, ApJ, 604, 18
Zentner A. R., Bullock J. S. 2003, ApJ, 598, 49
Zolotov A., Brooks A. M., Willman B. et al. 2012, ApJ, 761, 71 (Z12)

Appendix. THE MODEL

The model used in the paper was already described in Del Popolo (2009)(DP09) and Del Popolo (2012a,b) (DP12a, DP12b) (see also Del Popolo 2002; Cardone et al. 2011a,b). Here, we give a summary.

The model, described in DP09, DP12a and DP12b, is an improvement to the spherical infall models (SIM) already discussed by several authors (Gunn & Gott 1972; Bertschinger 1985; Hoffman & Shaham 1985; Ryden & Gunn 1987; Ascasibar et al. 2004; Williams et al. 2004)[4].

While previous authors studied how the basic SIM of Gunn & Gott (1972) is changed by introducing one effect at a time, as (a) just random angular momentum (e.g., Williams et al. 2004), (b) just adiabatic contraction (e.g., Blumenthal et al. 1986; Gnedin et al. 2004; Klypin et al. 2002; Gustafsson et al. 2006), or (c) just the effect of dynamical friction of DM and stellar clumps on the halo (El-Zant et al. 2001, 2004; Romano-Diaz et al. 2008), in our model the above effects (adiabatic contraction, dynamical friction, random angular momentum) and other effects (ordered angular momentum, gas cooling, star formation (DP09; De Lucia & Helmi 2008; Del Popolo & Gambera 1999, 2000) are all simultaneously taken into account.

As already reported, Gunn & Gott (1972) studied the self-similar collapse in an expanding universe, until "shell crossing"[5]. The evolution after "shell crossing" was studied by Gunn (1977). In the SIM, a spherical perturbation is divided into spherical shells and its evolution is followed in time.

One initially calculates the density profile at turn-around, $\rho_{\rm ta}(x_m)$, (Peebles 1980; White & Zaritsky 1992; Hoffman & Shaham 1985), assuming mass conservation and no "shell-crossing". Then, after shells start to cross, the final density profile is obtained assuming that the central potential varies adiabatically (Gunn 1977; Fillmore & Goldreich 1984), leading to

$$\rho(x) = \frac{\rho_{\rm ta}(x_m)}{f(x_i)^3}\left[1+\frac{d\ln f(x_i)}{d\ln g(x_i)}\right]^{-1}, \tag{7}$$

where $f(x_i) = x/x_m$ is the collapse factor, and the turn-around radius of a shell, x_m, is a monotonic increasing function of x_i, given by

$$x_m = g(x_i) = x_i \frac{1+\overline{\delta}_i}{\overline{\delta}_i - (\Omega_i^{-1}-1)}, \tag{8}$$

$\overline{\delta}_i$ being the density excess inside the shell (see Appendix A of DP09).

[4] Changes to the spherical collapse introduced by dark energy were studied in Del Popolo, Cardone & Belvedere (2013a), Del Popolo, Pace & Lima (2013b,c), Del Popolo et al. (2013d).

[5] After a shell reaches the turn-around radius it starts to collapse encountering the inner shells which are expanding or recollapsing giving rise to crossing of distinct shells.

In our model, we consider systems with DM and baryons. The way in which they were introduced and how we fixed their distribution in our study was discussed in Appendix E of DP09.

The baryon fraction was fixed as in McGaugh et al. (2010). The detected baryonic fraction, $f_{\rm d}$, is given by

$$f_{\rm d} = (M_{\rm b}/M_{500})/f_{\rm b} = F_{\rm b}/f_{\rm b}, \tag{9}$$

where $F_{\rm b} = M_{\rm b}/M_{500}$ is the baryonic fraction, and $f_{\rm b} = 0.17 \pm 0.01$ (Komatsu et al. 2009) is the universal baryon fraction.

During the evolution of the perturbation and its collapse, a random angular momentum, $j(r,\nu)_{\rm rand}$, is generated by random velocities (Ryden & Gunn 1987). Usually, in the SIM papers in which angular momentum is taken into account, only the random angular momentum is considered and assigned at turn-around (Le Delliou & Henriksen 2003; Ascasibar et al. 2004) as

$$j_{\rm rand} = j_* \propto \sqrt{GMr_m}, \tag{10}$$

or obtained by the random inner motions to the proto-structure (Ryden & Gunn 1987; Avila-Reese et al. 1998; Williams et al. 2004; Del Popolo & Kroupa 2009). Instead of directly assigning $j_{\rm rand}$, one can express it in terms of the ratio of pericentric, $r_{\rm min}$, to apocentric, $r_{\rm max}$, radii, $e = \left(\frac{r_{\rm min}}{r_{\rm max}}\right)$ (Avila-Reese et al. 1998), which is constant, and approximately equals 0.2 in N-body simulations[6]. A more detailed analysis shows that particle orbits tend to become more radial when they move to the turn-around radius, and, moreover, eccentricity depends from the dynamical state of the system, so that

$$e(r_{\rm max}) \simeq 0.8(r_{\rm max}/r_{\rm ta})^{0.1}, \tag{11}$$

for $r_{\rm max} < 0.1 r_{\rm ta}$, (Ascasibar et al. 2004). Random angular momentum is modeled through the Avila-Reese et al. (1998) method with the Ascasibar et al. (2004) correction.

The other form of angular momentum is the "ordered angular momentum", $h(r,\nu)$[7], produced by the tidal torque of the large-scale structure on the proto-structure (Hoyle 1949; Peebles 1969; White 1984; Ryden 1988; Eisenstein & Loeb 1995; Catelan & Theuns 1996). The total specific angular momentum, $h(r,\nu)$, is obtained by integrating the tidal torques, $\tau(r)$, over time (e.g., Ryden 1988, Eq. 35).

In our model, gas forms clumps, which exchange angular momentum through dynamical friction with dark matter.

A formula often used to describe this force is the Chandrasekhar's formula (Chandrasekhar 1943), and a more general treatment is that of Kandrup (1980). In the last case, the force per unit mass is given by

$$F = -\mu v = -\frac{4.44[GM_{\rm a}n_{\rm ac}]^{1/2}}{a^{3/2}N}\log\{1.12N^{2/3}\}v, \tag{12}$$

where v is the velocity, $n_{\rm ac}$ are the field particles comoving number density, N is the number of field particles in the system, and a is the expansion parameter.

[6] A value $e \simeq 0.2$ produces density profiles close to the NFW model. In Avila-Reese et al. (1998) it was fixed at 0.3.

[7] The peak height ν is defined as $\nu = \delta(0)/\sigma$, where $\delta(0)$ is the central overdensity value, and σ is the density field mass variance (Eq. B12 in DP09; see also Del Popolo & Gambera 1996).

In order to calculate the dynamical friction force it is necessary to know the number and distribution of field particles (substructure). As already reported, in the ΛCDM model, structure forms in a hierarchical bottom-up way. Halos contain subhalos, and the latter contains sub-subhalos (e.g., VL2 simulation). The subhalos cumulative mass function can be approximated as $M_{\rm sub} = 0.0064(M_{\rm sub}/M_{\rm halo})^{-1}$ to masses of $M_{\rm sub} = 4 \times 10^6 M_{\odot}$ (Diemand et al. 2007; Hiotelis & Del Popolo 2006; Hiotelis & Del Popolo 2013).

In our model, gas forms clumps, which exchange angular momentum through dynamical friction with dark matter. The mass of the clumps, $m_{\rm clump}$, is $m_{\rm clump} \simeq 0.01 M_{\rm halo}$, similarly to the clumps in the Cole et al. (2011) simulations. Evidence for the existence of these clumps comes from observations of galaxies at high redshift (Elmegreen et al. 2004, 2009; Genzel et al. 2011) which are found to show clumpy structures usually refereed to as "clump clusters" and "chain galaxies". Inoue & Saitoh (2011) showed through SPH simulations that these clumps are responsible for the cusp to core transformation in a fashion similar to what is described in this paper.

A fundamental "recipe" in galaxy formation is adiabatic contraction (AC) of DM haloes, produced by the baryon condensation in the centers of proto-structures. AC produces a steepening of the DM density profile (Blumenthal et al. 1986; Gnedin et al. 2004; Gustafsson et al. 2006) when baryons cool dissipatively and collapse to the proto-structure center, giving rise to a final baryonic mass distribution $M_{\rm b}(r) = M_* + M_{\rm gas}$, where $M_{\rm gas}$ is the gas mass and M_* is that of stars. The AC was calculated solving recursively the equation involved (Spedicato et al. 2003).

The structure formation in our model can be summarized as follows. The galaxy formation starts with the proto-structure in its linear phase, containing DM and gas. In our model, the baryons are initially in the form of a diffuse gas, with the previously quoted baryonic fraction. In order to follow the structure formation, we divide the proto-structure into mass shells made of DM and baryons. The proto-structure evolution is followed in the expansion phase, until turn-around, and in the following collapse by means of the SIM. As is known, DM collapse earlier than baryons to form the potential wells in which baryons fall. Baryons are subject to radiative processes with the formation of clumps, which collapse to the halo center condensing into stars, as described in Li et al. (2010, Sect. 2.2.2, 2.2.3), De Lucia & Helmi (2008), respectively. During the baryon infall phase, DM is compressed (AC). At this epoch the density profile of the proto-structure steepens. In their travel towards the center, baryon clumps are subject to DF from the less massive DM particles. This produces a predominant motion of DM particles outwards. The effect of the previous mechanism is amplified by the angular momentum acquired by the proto-structure through tidal torques (ordered angular momentum) and by random angular momentum. The cuspy profile is flattened to a cored one.

Our model is able to deal with the baryonic processes shaping the inner structure of galaxy clusters (and galaxies). It has become possible to predict in advance of SPH simulations (e.g., Governato et al. 2010, 2012; Martizzi et al. 2012) the correct shape of the density profiles of clusters (DP12a) and galaxies (DP09; Del Popolo & Kroupa 2009; DP12b) and correlations among several quantities in clusters of galaxies (DP12a) observed later in Newman et al. (2013a,b). The model also predicts correctly that the inner slope of the density profiles depends on the halo mass (Del Popolo 2010, 2011), later seen in the SPH simulations of Di Cintio et al. (2014).